Ray Lougeay
Department of Geography
State University College
Geneseo, NY 14454

Landsat Thermal Imaging of Alpine Regions

The thermal data are shown to provide a rendition of topographic texture lacking in other spectral bands of Landsat data.

Abstract: *Satellite-borne thermal data from Landsat are shown to be of utility in alpine regions. Even the highly degraded Landsat-3 thermal data are shown to contain information which aids in the interpretation of imagery depicting highly glacierized landscapes with extreme topographic texture. Comparison is given between Landsat-3 visible (MSS band 5, 600-700 nm) and thermal infrared (MSS band 8, 10,400-12,600 nm) images. Thermal patterns displayed on the Landsat thermal image are compared with ground level observations of radiometric emittance. The thermal data are shown to provide a rendition of topographic texture lacking in other spectral bands of Landsat data.*

Introduction

Since 1972, remotely sensed imagery from Landsat-1 and Landsat-2 have been used extensively, providing the backbone of satellite-based Earth imagery for various remote sensing applications. These platforms have enabled researchers to employ remotely sensed data for the investigation of a wide variety of problems in the physical and social sciences. Most of these studies have involved identification and mapping of phenomena at a small map scale, usually interpolating information between ground level sampling points which have been studied intensively. Of the various data recording systems aboard these Landsat vehicles, data from the four spectral bands of the multispectral scanner (MSS) have proved most useful, far exceeding any original expectations of consistent quality and absolute quantity of demonstrated applications.

With the launch of the Landsat-3 satellite remote sensing system in March of 1978, remotely sensed thermal imagery became readily available. Unfortunately, the Landsat-3 thermal imaging system experienced many problems, which resulted in very coarse spatial and thermal resolution. The thematic mapper, to be launched aboard Landsat-D′, should provide high quality thermal data. This paper addresses the potential utility of Landsat thermal imagery for the study of alpine regions. More specifically, imagery covering a small portion of the Alaskan Wrangell Mountains is analyzed with reference to extensive ground level data collected during the early summer of 1978, approximately four months after the launch of Landsat-3. Although Landsat-3's thermal imaging system did not produce imagery of as high a quality as originally anticipated, that which was provided does, at least, show the potential for this type of imaging system. The characteristic extremes of relief, plus various cover types and surface materials present within an alpine scene, produce greater ranges of surface temperatures (and emittance) than might be displayed in a scene with greater homogeneity.

The remote sensing community eagerly awaited data from the new, and experimental, thermal imaging system aboard Landsat-3. This thermal imaging system consisted of a fifth channel on the multispectral scanner, with a spectral sensitivity between 10,400 and 12,600 nanometres. Data acquired with this system provide imagery of terrestrial emittance which can be compared with pat-

Photogrammetric Engineering and Remote Sensing,
Vol. 48, No. 2, February 1982, pp. 269-273.

0099-1112/82/4802-269$02.25/0

terns of reflected solar energy displayed in the visible and near-visible infrared spectral bands of the Landsat multispectral scanners (see Table 1).

Unfortunately, the thermal imaging system aboard Landsat-3 did not provide data of as high a quality as originally hoped for. This was due to a series of system malfunctions. During the summer and fall of 1978 many members of the remote sensing community were frustrated to learn that the Landsat thermal system was not operating correctly. This system operated in its crippled mode for over one year, while the remaining bands of Landsat-3's multispectral scanner and the return beam vidicon system continued to produce quality data.

Landsat thermal imagery is available, although its quality has been degraded. The systems problems associated with the thermal sensing system aboard Landsat-3 are reflected in the quality of the imagery. Both thermal and spatial resolution were affected. After the first outgassing cycle of the thermal detector in mid-March 1978, the thermal resolution of the Landsat-3 system was approximately 1.2°C. This was better than the 1.5°C resolution of prelaunch specifications. This thermal sensitivity decreased to 2.5°C within the first week of operation due to the formation of condensation on the detector window. Outgassing cycles were performed approximately every two weeks after 21 March 1978. With each outgassing the thermal resolution improved, but not to the original level of the cycle before. As the signal-to-noise ratio became increasingly greater, the thermal imaging system was eventually turned off in the spring of 1979.

The spatial resolution of the thermal data from Landsat-3 is also less than originally anticipated. A partial failure of the thermal imaging system necessitated that the data from one scan line overlap to the next when processed. The best thermal data from Landsat-3 is that obtained soon after launch. However, problems affecting the thermal imaging system did not affect the high quality of imagery produced by the other spectral bands of the multispectral channels aboard Landsat-3. Also, the Landsat-3 return beam vidicon (RBV) system has operated well. While this system has a finer spatial resolution than the multispectral scanner, RBV data are limited to a single spectral band of reflected electromagnetic radiation (500-750 nm), similar to MSS bands 4 and 5.

Background

Previous work, by the author, in Alaska's Wrangell Mountains has involved the detection of moraine-covered glacier ice in the terminal regions of large alpine glaciers, which flow off the flanks of this mountain massif (Lougeay, 1979). Hundreds of square kilometres of active moraine-covered glacier ice exist within this region. It was found that Landsat spectral bands 5, 7 (Table 1), and, to an extent, false color composite imagery from existing Landsat multispectral data proved most useful in mapping glacial margins and large masses of active, but buried, glacier ice. Signal contrasts between bare detritus and vegetation cover were most strongly pronounced on band 5, while band 7 displayed stronger contrasts between the microtopographic texture of the moraine-covered ice masses and adjacent detrital surfaces of talus or outwash. Radiometric data from airborne overflights were used to prepare thermal emittance maps which simulated Landsat thermal imagery (MSS band 8). Information from these simulations, combined with ground level observations and the overflights, has served to augment the information available from the visible and near-visible Landsat imagery. The thermal imagery of MSS band 8 was found to be of limited use by itself due to its coarse spatial and thermal resolution. Ground data did show that, when the mantle of morainic detritus is thinner than the diurnal thermal damping depth, strong signal contrasts between ice cored moraines and dry glacial drift deposits are present. In addition, simulations of Landsat-3 thermal imagery did display strong contrasts between areas of relatively different surface flow activity within the mass of buried ice, due to varying thickness of morainic mantle (Lougeay, 1974; Lougeay, 1979).

Table 1

MSS Band No.	Spectral Sensitivity	
4	500–600 nm	Reflected green sunlight (visible)
5	600–700 nm	Reflected red sunlight (visible)
6	700–800 nm	Reflected infrared solar energy
7	800–1,100 nm	Reflected infrared solar energy
8	10,400–12,600 nm	Thermal infrared terrestrial emittance

Discussion

Figure 1 displays an 808 square kilometre area of the Wrangell Mountains. This scene is a small portion of a standard Landsat MSS band 5 image, showing patterns of reflected electromagnetic radiation from the red regions of the visible spectrum (600-700 nm). Within the scene one can see the eastern flanks of Mt. Regal (a), which reaches a summit elevation of 4,220 metres. Prominent glaciers in the area are the Regal (b), Nizina (c), West Fork (d), Root (e), and the Kennicott (f).

Snow and bare glacier ice appear white in Figure 1, while the moraine-covered portions of the glaciers appear as a medium gray and blend into the bedrock and talus slopes of adjacent mountain walls. Areas of alpine tundra are indistinguishable from bedrock and talus, but the upper tree line of the subarctic coniferous forest is quite obvious. This coniferous forest canopy reflects very little visible light and is quite dark on the band 5 image. The darkest tones in the scene are areas of shadow cast by the steep mountain walls and relatively low solar elevation of this high latitude location. The floodplain of the Nizina River (1), consisting of a braided melt water channel and gravel bars, appears as a light gray in Figure 1.

The Landsat-3 thermal image (band 8) of the same scene as Figure 1 is shown in Figure 2. This thermal image displays a very different pattern of gray tones. The coarse resolution scan lines from the original film transparency are quite apparent. Variations in gray tones represent radiometric emittance from the Earth's surface. The amount of electromagnetic energy emitted from the surface is a direct function of surface temperature.[1] In this case the lighter tones correspond to warmer surface temperatures. The cold snowpack in the higher elevations of Mount Regal (a) is very dark on this thermal image. Southeast facing bedrock and talus slopes, which receive incident sunlight almost perpendicularly, are quite warm and appear very bright. This image was obtained at 10:16 hours, with the sun 38 degrees above the horizon at an azimuth of 154 degrees. While many have observed that Landsat-3 thermal imagery is of limited use, at this coarse scale of relief the thermal data do provide some topographic information which is not readily available from the other Landsat spectral bands.

There are two primary factors which produce apparent patterns of temperature variation at the Earth's surface. These are either variation in surface material type, or changing slope and exposure (see footnote). As slope characteristics change, the amount of incident solar energy available to warm the surface changes. This available heat energy is then used to warm the surface to varying degrees, dependent upon the thermal parameters of the surface materials and available heat sinks (e.g., moisture for evaporation). The works of Kahle (1977), Gillespie and Kahle (1977), and Dozier and Frew (1981) are cited as reference to methods of modeling slope and atmospheric corrections for remotely sensed thermal data over rugged terrain. Variations in slope and exposure are quite evident when comparing Figures 1 and 2. These topographic variations explain most of the gray tone patterns present in Figure 2. In fact, the Landsat thermal image provides a rendition of gross topographic structure which is lacking in other Landsat images, such as those depicted in Figure 1.

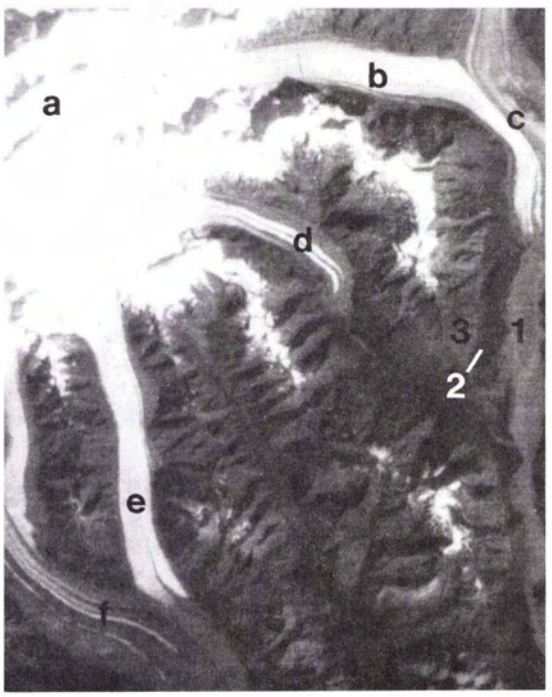

FIG. 1. Landsat-2 MSS band 5 (600-700 nm), image #E-1422-20212-5, 18 September 1973. Approximately 61°40′ North latitude, 142°40′ West longitude. Image width represents 25 kilometres.

[1] Thermal infrared radiant energy emitted from the ground surface is expressed by the equation: $R = e\sigma K^4$, where R is the emittance in ly/min, e is the emissivity of the surface material, σ is the Stefan-Boltzman constant (8.132×10^{-11}), and K is the absolute surface temperature. Only differences in surface temperature or emissivity will produce variations in emittance. Surface temperature is a direct product of the surficial energy budget: $R_{net} = \pm S \pm E \pm G$. Here R_{net} is the net radiant energy available at the surface. S is the convective heat transfer betweeen the surface and atmosphere, E is the latent heat transfer of evaportranspiration and condensation, and G is the conductive transfer of heat to and from the surface. R_{net} is the result of the surface radiant energy balance, and is strongly controlled during daylight hours by available insolation.

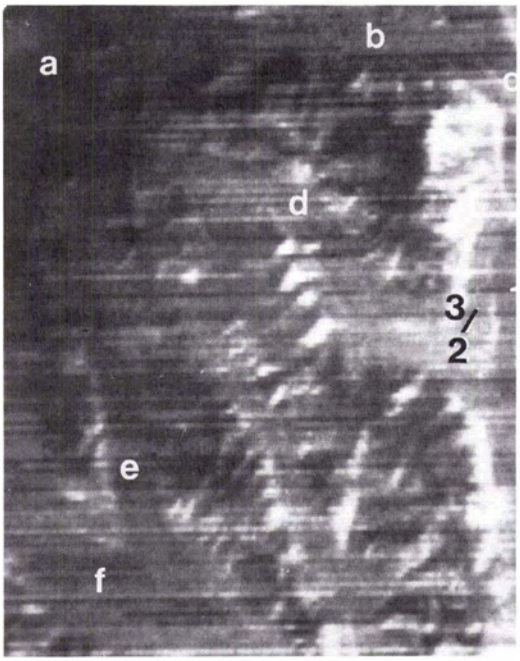

FIG. 2. Landsat-3 MSS band 8 (10,400-12,600 nm), image #E-30046-20161-8, 20 April 1978. Approximately 61°40′ North latitude, 142°40′ West longitude. Image width represents 25 kilometres.

Variations in surface materials, and cover type, do affect surface temperature and are evidenced in the thermal image (Figure 2). Table 2 shows various radiometric surface temperatures measured from airborne overflights in this region. These flights are flown in the late morning of a clear day under weather conditions very similar to those present when the Landsat thermal image (Figure 2) was obtained. In Figure 1 the reflective characteristics of the Nizina floodplain (1), coniferous forest (2), and the alpine zone above tree line (3) can be seen. These features are also apparent in the thermal image (Figure 2). The composite temperature of the floodplain and glacial meltwater appears somewhat cooler than the forest canopy. Data from Table 2 might lead one to expect this thermal pattern during the late ablation season when most of the channels are filled with meltwater. The forest canopy is cooler than the alpine zone above. This is also explained by the data in Table 2; however, one does not expect the talus, tundra, and bedrock of the alpine zone to be quite so warm. In the situation of point 3, the southeast facing slope is much warmer than other slopes of the alpine zone due to extreme solar heating. Many bright spots in Figure 2 correspond to topographic facets which have received maximum insolation as a function of their orientation to the incoming rays of the sun. The warm linear pattern which corresponds to the western lateral edge and near-terminus of the Nizina glacier (c) in Figures 1 and 2 is of particular interest. This warm linear feature on Figure 2 is a bluff which has been over-steepened by the erosive action of the glacier. The emittance contrast between the bluff and adjacent lateral moraine of the Nizina Glacier provides delineation of the glacier's margin.

TABLE 2. GENERALIZED RADIOMETRIC EMITTANCE VALUES
(as observed from airborne overflights and adjusted for slope variation)

Surface/Cover Type*	Emittance (ly/min)	Apparent Temperature** (°C)
Coniferous Forest	0.47	3
Alpine Tundra	0.48	4
Bedrock	0.48	4
Talus	0.48	4
Outwash Gravels	0.51	5
Ablation Moraine	0.48–0.49	4–6
Glacier Ice	0.45	0
Glacial Meltwater	0.45	0
Snow/Firn	<0.45	<0

* Surfaces have been adjusted to horizontal
** Emissivity assumed to be 1.0

The glaciers which are relatively obvious in Figure 1 are almost totally lost in the thermal image (Figure 2). The surface temperatures of the glacial ablation zones, and associated surfaces of ablation moraine, all appear as a medium gray tone. Variations in emittance between these surfaces and adjacent features are not great enough to be obvious, given the coarse thermal resolution of the Landsat-3 thermal imaging system. The Root Glacier (e), which appears darker on the thermal image, displays colder temperatures and lower levels of emittance. This is due to morning shading of the glacier by mountain walls immediately to the east. Colder surface temperatures of the high elevation glacier accumulation zones, such as the upper slopes of Mt. Regal (a), appear very dark on the thermal image (Figure 2).

Remotely sensed thermal data from the Landsat thermal imaging systems are of use in alpine areas where extremes of topography and ambient temperatures are such that the coarse spatial and thermal resolution of the system does not mask the features under study. The thermal imagery is perhaps most useful in depicting areas of relief with relatively homogeneous surface covers, especially where the reflectance is high and the solar sensitive detectors have been saturated. An example of this is found in the greater detail to be seen in the northwestern section of Figure 2 as compared to Figure 1. Here the high albedo snow surface of Mt. Regal has saturated band 5, but the variations in slope have produced varying emittance values apparent in band 8.

Conclusions

At the very least, the available Landsat-3 thermal imagery has shown the potential for application of data from future thermal remote sensing systems. Unfortunately, only the degraded Landsat-3 data are now readily available to the general public. However, satellite remotely sensed high quality thermal data have been acquired by the NASA Thermal Heat Capacity Mission (HCMM) (National Space Science Data Center, 1981). Limited amounts of these data are available to interested researchers. Also, some NOAA thermal imagery is available with a spatial resolution as fine as two kilometres. Landsat-D′ will carry a full array of sensors within the newly designed thematic mapper. Thermal imagery from this system should have a much finer spatial and thermal resolution than that of Landsat-3. This discussion of Landsat-3 thermal imagery suggests that future remotely sensed thermal data may provide information previously unavailable from satellite remote sensing systems depicting only the visible and near-visible infrared portion of the electromagnetic spectrum. Greatest potential seems to lie within the realm of analyzing gross patterns of topographic texture, once ground level observations have provided enough information about signal contrasts present as a function of varying surfaces and cover types.

References

Dozier, J., and J. Frew, 1981. Atmospheric Corrections to Satellite Radiometric Data over Rugged Terrain. *Remote Sensing of Environment* 11(3):191-205.

Dozier, J., and S. I. Outcalt, 1979. An Approach Toward Energy Balance Simulation Over Rugged Terrain. *Geographical Analysis* 11(1):65-85.

Gillespie, A. R., and A. B. Kahle, 1977. Construction and Interpretation of a Digital Thermal Inertia Image. *Photogrammetric Engineering and Remote Sensing* 43(8):983-1000.

Kahle, A. B., 1977. A Simple Thermal Model of the Earth's Surface for Geologic Mapping by Remote Sensing. *Journal of Geophysical Research* 82(11): 1673-1680.

Lintz, J., and D. Simonett, 1976. *Remote Sensing of Environment.* Addison-Wesley Co., Reading, Massachusetts.

Lougeay, R., 1972. Patterns of Surface Temperature in the Alpine/Periglacial Environment as Determined by Radiometric Measurements. In *Icefield Ranges Research Project Scientific Results,* Volume III. American Geographical Society and Arctic Institute of North America, Washington, D.C., pp. 163-176.

———, 1974. Detection of Buried Glacial and Ground Ice with Thermal Infrared Remote Sensing. In *Advanced Concepts and Techniques in the Study of Snow and Ice Resources.* H. S. Santeford and H. L. Smith, eds., National Academy of Science, Washington, D.C., pp. 487-494.

———, 1979. Potentials of Mapping Buried Glacier Ice with LANDSAT Thermal Imagery. In *Satellite Hydrology,* American Water Resources Association, Proceedings of the 5th Annual Pecora Symposium, Sioux Falls, South Dakota, pp. 189-192.

National Aeronautics and Space Administration, 1976 and 1978. *Data Users Handbook.* Goddard Space Flight Center, Greenbelt, Maryland.

National Space Science Data Center, 1981. Thermal Infrared Data from the Heat Capacity Mapping Mission. *Remote Sensing of Environment* 11(1):77-79.

Outcalt, S., 1972. The Simulation of Subsurface Effects of the Diurnal Surface Thermal Regime in Cold Regions. *Arctic* 25(4):306-308.

Outcalt, S., C. Goodwin, G. Weller, and J. Brown, 1975. *A Digital Computer Simulation of the Annual Snow/Soil Thermal Regime at Barrow, Alaska.* USA CRREL Research Report 331. (Also *Water Resources Research* 11:709-715.)

Price, John, 1981. The Contribution of Thermal Data in LANDSAT Multispectral Classification. *Photogrammetric Engineering and Remote Sensing* 47(2):229-236.

Reeves, Robert G. (ed.), 1975. *Manual of Remote Sensing.* American Society of Photogrammetry, Falls Church, Va., 2144 p.

Richason, B., Jr., ed., 1978. *Introduction to Remote Sensing of the Environment.* Kendall/Hunt Publishing Co., Dubuque, Iowa.

(Received 3 April 1981; accepted 15 August 1981; revised 13 September 1981)